SINGULAR AND HYPERSINGULAR INTEGRAL EQUATIONS IN FLUID–STRUCTURE INTERACTION ANALYSIS

VASYL I. GNITKO[1], ARTEM O. KARAIEV[2*], KYRYL G. DEGTYARIOV[1],
IVAN A. VIERUSHKIN[1] & ELENA A. STRELNIKOVA[1,2†]
[1]A. Podgorny Institute of Mechanical Engineering Problems of the Ukrainian Academy of Sciences, Ukraine
[2]V.N. Karazin Kharkiv National University, Ukraine

ABSTRACT

The paper presents new computational techniques based on coupled boundary and finite element methods to study fluid–structure interaction problems. Thin shells and plates are considered as structure elements interacting with an ideal and incompressible liquid. To describe the motion of both structural elements and the fluid, the basic relations of the continuous mechanics are incorporated. The liquid pressure is determined by applying the Laplace equation. Two kinds of boundary value problems are considered corresponding to one-sided and two-sided contact of structural elements with the liquid. Integral equations for numerical simulation of pressure are obtained. For a two-sided contact of the structural element with the liquid, hypersingular integral equations are received, whereas singular integral equations with logarithmic singularities describe the problems of one-sided contact. Considering the structure axial symmetry, the integral equations are reduced to one-dimensional ones. The finite element method for determining modes and frequencies of the elastic structure coupled with boundary element method for the hypersingular integral equation is implemented to find the fluid pressure on the structure element with two-sided contact with the liquid. The liquid pressure evaluation in axisymmetric problems is reduced to one-dimensional integral equations with kernels in the form of elliptic integrals. The effective technique is developed for numerical simulation of obtained singular integrals. The same technique is extended to hypersingular integral equations. The frequencies and modes of structure vibrations taking into account the added masses of the liquid are obtained. Thin circular plates and shells of revolution are considered as structure elements in numerical simulations. The accuracy and reliability of the proposed method are ascertained.

Keywords: fluid–structure interaction, boundary and finite element methods, singular and hypersingular integral equations, free vibrations, fluid-filled elastic shells.

1 INTRODUCTION

Problems of fluid–structure interaction (FSI) have been of great interest to many scientists and practicing engineers in recent decades. A distinguishing feature of the structure elements is that they operate in interaction with air or water. Owing to this, to define strength characteristics, one must solve coupled fluid and aero elasticity problems, i.e. determine stress and strain fields and vibration frequencies taking into account fluid or gas pressure acting on the elastic body. Among these problems there are topical issues of estimation of dynamic characteristics of Kaplan and Francis turbine wheels [1], blades and covers [2], steam and wind turbine units [3], [4], micro and nanotubes [5], fuel tanks [6] and oil storages [7]. FSI problems are conventionally divided into two classes. The first one includes the problems of determining the dynamic characteristics of structures with liquids, when the structure surfaces are in one-sided contact with the liquid. Faltinsen et al. [8], Strelnikova et al. [9] and Zhou-Bowers and Rizos [10] devoted to these problems are concerned with liquid sloshing in rigid shell systems. The vibrations of elastic structures containing liquids are

* *ORCID: https://orcid.org/0000-0003-3176-8496*
† *ORCID: http://orcid.org/0000-0003-0707-7214*

WIT Transactions on Engineering Sciences, Vol 134, © 2022 WIT Press
www.witpress.com, ISSN 1743-3533 (on-line)
doi:10.2495/BE450061

analyzed in Avramov [5], Boyko et al. [11], Strelnikova et al. [12] and Saghi et al. [13]. A second class is concerned with two-sided contact with liquids in simulating dynamic characteristics for blades of powerful wind turbines [4], aircraft wings [14], etc. For irrotational flows of ideal and incompressible liquids, the most effective techniques are elaborated using singular and hypersingular integral equations with boundary element methods (BEM) for their numerical implementation [15], [16]. In this paper hypersingular integral equations are received at the two-sided contact simulation in FSI problems, whereas singular integral equations with logarithmic and Cauchy-type singularities describe one-sided contact problems.

2 PROBLEM STATEMENT AND BASIC RELATIONS

The basic relations of continuous mechanics are used to describe the motion of both elastic structures and fluids [16]. Suppose there is an elastic body occupying the region Ω with the boundary Γ. Suppose also that given volume and surface forces act on the body. In addition, a part of the body surface is in contact with the liquid. All continuous medium models provide methods to estimate stress and strains fields σ_{ij}, ε_{ij}, displacements u_i, (i, j = 1,2,3), pressure p, and density ρ, depending on time. For unambiguous definition of σ_{ij}, ε_{ij}, u_i, p, and ρ, it is necessary to set additional relationships between stresses and strains, or between stresses and strain rates. If an elastic body is studied, then the relationship between strains and stresses is described by Hooke's law. To describe the fluid, the relationship between stresses and strain rates is specified.

2.1 Basic equations of elastic body motion

To solve equations of elastic body motion, the method of weighted residuals is used [16]. The unknowns are given as series of finite functions $\{\psi_n\}|_{n=1}^{N_1}$, as trial ones, the functions from the same basis are incorporated. After integration of the received relation on volume and reducing some of the volume integrals to surface ones, the finite-element formulation of the problem is received as follows [16]

$$[\mathbf{M}_S]\ddot{\boldsymbol{u}}^e + [\mathbf{C}_S]\dot{\boldsymbol{u}}^e + [\mathbf{K}_S]\boldsymbol{u}^e = \{\boldsymbol{f}_S\} + \{\boldsymbol{f}_{pr}\}, \tag{1}$$

where $[\mathbf{M}_S], [\mathbf{C}_S], [\mathbf{K}_S]$ are mass, damping, and stiffness matrices, respectively, $\{\boldsymbol{f}_S\}$ is for given forces acting on the elastic body, $\{\boldsymbol{f}_{pr}\}$ is for pressure on wetted surfaces of the elastic body, $\boldsymbol{u}^e$ are the elastic displacements.

2.2 Basic relations of liquid motion

To determine the vector $\{\boldsymbol{f}_{pr}\}$, the initial-boundary value problem in fluid mechanics is formulated hereinafter. The liquid is supposed to be compressible and viscous, and its movement is vortex-free. Assume that the perturbations of the fluid pressure due to the motion of the elastic body are small, i.e. the problem is considered in a linear formulation. The general laws of fluid mechanics are in use, namely, the mass conservation law (continuity equation) and momentum conservation law

$$\frac{\partial \rho}{\partial t} = -\operatorname{div}(\rho \mathbf{V}_f) + Q, \quad \rho \frac{d\mathbf{V}_f}{dt} = \rho \mathbf{b} + \operatorname{div}(\boldsymbol{\sigma}_f), \tag{2}$$

where $\mathbf{V}_f$ is the fluid velocity vector, ρ is a liquid density, Q is for mass sources, t is time, $\mathbf{b}$ is for volume forces. To determine the components of the stress tensor, the following hypothesis is incorporated

$$\boldsymbol{\sigma}_f = -p\mathbf{I} + \mathbf{T}, \quad \mathbf{T} = 2\mu\left(\dot{\mathbf{S}} - \frac{1}{3}\left(\operatorname{div}\mathbf{V}_f\right)\right), \tag{3}$$

where $\mathbf{I}$ is an identity tensor, $\dot{\mathbf{S}}$ is the strain-rate deviator, μ is the viscosity coefficient.

Using the equations of state $p = p(\rho)$, $\frac{\partial p}{\partial \rho} = c^2$, the following approximate relations are received

$$\operatorname{div}\mathbf{V}_f = -\frac{1}{\rho_l c^2}\frac{\partial p}{\partial t} + \frac{Q}{\rho_l}, \quad \frac{\partial \mathbf{V}_f}{\partial t} = -\frac{1}{\rho_l}\nabla p + \frac{4\mu}{3\rho_l}\left(-\frac{1}{\rho_l c^2}\frac{\partial p}{\partial t} + \frac{Q}{\rho_l}\right), \tag{4}$$

where ρ_l is the liquid density average value at linearization.

Suppose that the liquid is incompressible and non-viscous one, and there are no mass sources. Then

$$\operatorname{div}\mathbf{V}_f = 0, \quad \rho_l\frac{\partial \mathbf{V}_f}{\partial t} = -\nabla p. \tag{5}$$

It follows from eqn (5) that pressure p satisfies the Laplace equation, namely

$$\frac{\partial^2 p}{\partial x^2} + \frac{\partial^2 p}{\partial y^2} + \frac{\partial^2 p}{\partial z^2} = 0. \tag{6}$$

Note that pressure, or its overfall, is included in the right-hand side of eqn (1).

3 BOUNDARY VALUE PROBLEM FOR LIQUID PRESSURE EVALUATING

3.1 Mode superposition method

Suppose that the unknown displacements are presented as following series

$$\boldsymbol{u}^e(x,y,z,t) = \sum_{k=1}^{N} c_k(t)\boldsymbol{u}_k(x,y,z), \tag{7}$$

where $c_k(t)$ are unknown time-dependant coefficients, and $\boldsymbol{u}_k(x,y,z)$ are known functions. Functions $c_k(t)$ are usually considered as generalized coordinates. Using eqn (7), we transform eqn (1) into the next form

$$\sum_{k=1}^{N}\{\ddot{c}_k(t)[\mathbf{M}_S\boldsymbol{u}_k] + \dot{c}_k(t)[\mathbf{C}_S\boldsymbol{u}_k] + c_k(t)[\mathbf{K}_S\boldsymbol{u}_k]\} = \{\boldsymbol{f}_S\} + \{\boldsymbol{f}_{pr}\}. \tag{8}$$

Following the weighted residuals method [17], perform the dot product of eqn (8) sequentially on the functions $\boldsymbol{u}_l(x,y,z)$ and receive

$$[\mathbf{M}][\ddot{\boldsymbol{c}}] + [\mathbf{C}][\dot{\boldsymbol{c}}] + [\mathbf{K}][\boldsymbol{c}] = \{\tilde{\boldsymbol{f}}_S\} + \{\tilde{\boldsymbol{f}}_{pr}\}, \tag{9}$$

where

$$[\mathbf{M}] = \{(\mathbf{M}_S\boldsymbol{u}_k, \boldsymbol{u}_l)\}, [\mathbf{C}] = \{(\mathbf{C}_S\boldsymbol{u}_k, \boldsymbol{u}_l)\}, [\mathbf{K}] = \{(\mathbf{K}_S\boldsymbol{u}_k, \boldsymbol{u}_l)\},$$
$$\{\tilde{\boldsymbol{f}}_S\} = \{(\boldsymbol{f}_S, \boldsymbol{u}_l)\}, \{\tilde{\boldsymbol{f}}_{pr}\} = \{(\boldsymbol{f}_{pr}, \boldsymbol{u}_l)\}.$$

If $\{\tilde{\boldsymbol{f}}_S\} = \{\tilde{\boldsymbol{f}}_{pr}\} = 0$, then frequencies and modes of free vibrations for the structure without liquid added masses are defined. When $\{\tilde{\boldsymbol{f}}_S\} = 0$, we come to the problem of determining the frequencies and modes of the free vibrations of structural elements with added liquid masses.

3.2 Bilateral contact of the structural element with the liquid

If the bilateral contact of the structural element with the liquid is studied, then pressure overfall is needed to be considered on the wetted surfaces. As is mentioned above, the pressure satisfies Laplace's eqn (6). So, it is necessary to formulate boundary conditions for this equation. Suppose that the structural element is quite thin, so boundary conditions can be set at the middle surface of the element under consideration (Fig. 1(a)).

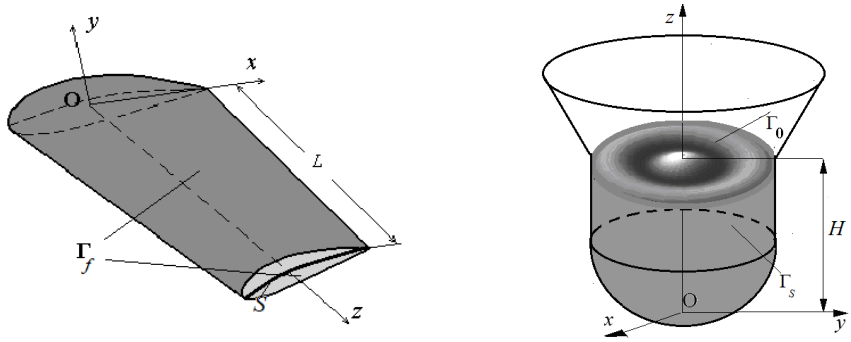

(a) (b)

Figure 1: Structure elements interacting with liquids.

First, the boundary no-penetration condition is formulated. For inviscid fluids it means equality of normal components of the fluid and solid velocities

$$(\dot{\boldsymbol{u}}^e, \mathbf{n}) = (\mathbf{V}_f, \mathbf{n}), \quad \frac{\partial p^{\pm}}{\partial \mathbf{n}} = -\rho_l(\ddot{\boldsymbol{u}}^e, \mathbf{n}) = -\rho_l \sum_{k=1}^{N} \ddot{c}_k(t)\,(\boldsymbol{u}_k, \mathbf{n}). \tag{10}$$

The normal derivative of the pressure p has to be continuous, but on the element surface S, the pressure has its overfall. Besides, the function p is harmonic, and satisfies Sommerfeld's condition at infinity. Noted, that the double layer potential has the required properties [16]

$$p(\mathbf{P}_0) = \frac{1}{4\pi} \iint_S \Gamma(\mathbf{P}) \frac{\partial}{\partial \mathbf{n}} \frac{1}{|\mathbf{P}-\mathbf{P}_0|} dS, \quad \mathbf{P} \in S, \tag{11}$$

where S is the area occupied by the structural element; $\mathbf{n}$ is the unit normal to the surface S, $\mathbf{P}$ and $\mathbf{P}_0$ are points with coordinates (x, y, z) and (x_0, y_0, z_0), respectively, the function $\Gamma(\mathbf{P})$ is the potential density, whereas $|\mathbf{P} - \mathbf{P}_0| = \sqrt{(x-x_0)^2 + (y-y_0)^2 + (z-z_0)^2}$ is the Cartesian distance between points $\mathbf{P}$ and $\mathbf{P}_0$.

Function (11) satisfies Laplace's eqn (6), has the continuous normal derivative, and a finite gap along the normal to the surface S, namely

$$p^+(\mathbf{P}_0) - p^-(\mathbf{P}_0) = \Gamma(\mathbf{P}_0), \quad \mathbf{P}_0 \in S. \tag{12}$$

Note that to determine the pressure overfall, it is necessary to find the unknown density $\Gamma(\mathbf{P})$. So, boundary condition (10) has to be satisfied. This leads to the following integral equation

$$\frac{\partial}{\partial \mathbf{n}_0} \frac{1}{4\pi} \iint_S \Gamma(\mathbf{P}) \frac{\partial}{\partial \mathbf{n}} \frac{1}{|\boldsymbol{P}-\boldsymbol{P}_0|} dS = -\rho_l(\ddot{\boldsymbol{u}}^e, \mathbf{n}_0), \quad \mathbf{P}, \mathbf{P}_0 \in S. \tag{13}$$

From eqn (10) one can receive that

$$\Gamma(\mathbf{P}) = \sum_{k=1}^{N} \ddot{c}_k(t)\,\Gamma_k(\mathbf{P}) \tag{14}$$

where functions $\Gamma_k(\mathbf{P})$ are satisfying the integral equations

$$\frac{\partial}{\partial \boldsymbol{n}_0}\frac{1}{4\pi}\iint_S \Gamma_k(\mathbf{P})\frac{\partial}{\partial \mathbf{n}}\frac{1}{|\boldsymbol{P}-\boldsymbol{P}_0|} = -\rho_l(\boldsymbol{u}_k, \mathbf{n_0}), \quad \mathbf{P}, \mathbf{P}_0 \in S. \tag{15}$$

Introducing the inverse operator $\mathbf{H}$ as $\Gamma_k(\mathbf{P}) = -\rho_l \mathbf{H}(\boldsymbol{u}_k)$, one can obtain the next relation for added masses in (9)

$$\{\tilde{\boldsymbol{f}}_{pr}\} = -\rho_l[\mathbf{H}][\ddot{\boldsymbol{c}}], \quad [\mathbf{H}] = \{\mathbf{H}\boldsymbol{u}_k, \boldsymbol{u}_l\}. \tag{16}$$

Thus, in eqn (10) for determining the modes and frequencies of structures at bilateral contact with the liquid, the vector $\{\tilde{\boldsymbol{f}}_{pr}\}$ is needed to be calculated by eqn (16). It would be noted that the indirect formulation of the boundary element method [16] is used here to calculate the fluid pressure overfall.

3.3 Unilateral contact of the structural element with the liquid

Let an elastic shell be partially filled with an ideal and incompressible liquid. At unilateral contact, it is necessary to evaluate the pressure in the liquid domain Ω_f. So, the boundary value problem is needed to be formulated for Laplace's eqn (6). Let $\Gamma_f = \Gamma_S \cup \Gamma_0$ be the boundary of Ω_f supposing that Γ_S is the shell wetted surface, and Γ_0 is the liquid free surface (Fig. 1(b)). At unilateral contact, the mode superposition method is also implemented. This leads to no-penetration condition (10) on the wetted surfaces, whereas kinematic and dynamic conditions are applied on the liquid free surface. From the dynamic condition, we have

$$p = \rho_l g \eta, \tag{17}$$

where the function η describes the free surface elevation over time.

According to the kinematic condition, fluid points that were initially on the free surface, remain on this surface throughout the whole movement. Let the free surface equation be $F(x, y, z, t) = z - \eta(x, y, t) = 0$. Considering time moment $t + \Delta t$, one can obtain

$$0 = \frac{dF}{dt} = \frac{\partial F}{\partial t} + \frac{\partial F}{\partial x}\dot{x} + \frac{\partial F}{\partial y}\dot{y} + \frac{\partial F}{\partial z}\dot{z} = -\frac{\partial \eta}{\partial t} - \frac{\partial \eta}{\partial x}V_x - \frac{\partial \eta}{\partial y}V_y + V_z. \tag{18}$$

So, the following approximate equations are valid on the free surface:

$$\frac{\partial \eta}{\partial t} = (\mathbf{V}_f, \mathbf{n}), \quad \frac{\partial^2 \eta}{\partial t^2} = \left(\frac{\partial \mathbf{V}_f}{\partial t}, \mathbf{n}\right) = \left(-\frac{1}{\rho_l}\nabla p, \mathbf{n}\right). \tag{19}$$

Using eqns (17) and (19), we receive

$$\eta = \frac{p}{\rho_l g}, \quad \left.\frac{\partial p}{\partial \mathbf{n}}\right|_{\Gamma_0} = -\frac{1}{g}\frac{\partial^2 p}{\partial t^2}. \tag{20}$$

Thus, the boundary value problem is formulated for evaluating the pressure as solution of eqn (6) under boundary conditions (10), (20). Note that the initial conditions are needed to be added. It is usually assumed that at initial time the fluid was at rest.

According to the weighted residual method, eqn (6) is multiplied by the test function w and then integrated by liquid volume Ω_f. In the boundary element method (BEM) unlike the

finite element method (FEM) integration by parts is performed twice, resulting in the weak boundary value problem formulation. Namely, using Green's first formula, we have

$$\iiint_{\Omega_f} \nabla^2 p \cdot w d\Omega_f = -\iiint_{\Omega_f} (\nabla p, \nabla w) d\Omega_f + \iint_{\Gamma_f} w(\nabla p, \mathbf{n})\, d\Gamma_f. \tag{21}$$

Applying the divergence theorem to eqn (21), we get

$$\iiint_{\Omega_f} \nabla^2 w \cdot p d\Omega_f = \iint_{\Gamma_f} p(\nabla w, \mathbf{n})\, d\Gamma_f - \iint_{\Gamma_f} w(\nabla p, \mathbf{n})\, d\Gamma_f. \tag{22}$$

Introduce trial functions in the form

$$U(\mathbf{P}, \mathbf{P}_0) = \frac{1}{|\mathbf{P} - \mathbf{P}_0|}. \tag{23}$$

It would be noted that

$$\nabla^2 U(\mathbf{P}, \mathbf{P}_0) = \delta(\mathbf{P} - \mathbf{P}_0), \tag{24}$$

where $\delta(\mathbf{P} - \mathbf{P}_0)$ is delta function. From (22), using weight residual method with trial functions (23), we receive singular integral equations

$$2\pi p(\mathbf{P}_0^k) = \iint_{\Gamma_f} \frac{\partial p}{\partial \mathbf{n}} \frac{1}{|\mathbf{P} - \mathbf{P}_0^k|} d\Gamma_f - \iint_{\Gamma_f} p \frac{\partial}{\partial \mathbf{n}} \frac{1}{|\mathbf{P} - \mathbf{P}_0^k|} d\Gamma_f, \quad k = 1,2 \ldots. \tag{25}$$

Taking into account boundary conditions (10), (20) we obtain

$$2\pi p(\mathbf{P}_0^k) + \iint_{\Gamma_f} p \frac{\partial}{\partial \mathbf{n}} \frac{1}{|\mathbf{P} - \mathbf{P}_0^k|} d\Gamma_f = \iint_{\Gamma_S} (\ddot{\mathbf{u}}_e, \mathbf{n}) \frac{1}{|\mathbf{P} - \mathbf{P}_0^k|} d\Gamma_S - \frac{1}{g} \iint_{\Gamma_0} \frac{\partial^2 p}{\partial t^2} \frac{1}{|\mathbf{P} - \mathbf{P}_0^k|} d\Gamma_0, \tag{26}$$

where $\mathbf{P}_0^k$, $k = 1,2 \ldots$ are collocation points.

Eqns (26) are singular equations with respect to the unknown pressure p.

4 SINGULAR AND HYPERSINGULAR INTEGRAL EQUATIONS IN AXISYMMETRIC PROBLEMS

4.1 Hypersingular integral equations

If the domain S in eqn (13) is a circle, then it is possible to reduce the two-dimensional hypersingular equation to one-dimensional. Let S be a circle on the xOy plane, namely $S = \{x, y: x^2 + y^2 \le R^2\}$.

Let receive the distance $|\mathbf{P} - \mathbf{P}_0|$ in cylindrical coordinates. We have $|\mathbf{P} - \mathbf{P}_0| = \sqrt{\rho^2 + \rho_0^2 + (z - z_0)^2 - 2\rho\rho_0 \cos(\theta - \theta_0)}$, where

$$x = \rho\cos\theta, \quad y = \rho\sin\theta, \quad z = z, \quad x^2 + y^2 = \rho^2,$$

$$x_0 = \rho_0\cos\theta_0, \quad y_0 = \rho_0\sin\theta_0, \quad z_0 = z_0, \quad x_0^2 + y_0^2 = \rho_0^2.$$

Introduce the following hypersingular operator

$$\mathbf{G}\Gamma = \frac{\partial}{\partial \mathbf{n}_0} \frac{1}{4\pi} \iint_S \Gamma(\mathbf{P}) \frac{\partial}{\partial \mathbf{n}} \frac{1}{|\mathbf{P} - \mathbf{P}_0|} dS. \tag{27}$$

Suppose that the function $\Gamma(\mathbf{P})$ does not depend on the circumferential coordinate θ, i.e. consider the problem in axially symmetric formulation. Taking into account the assumptions about the axial symmetry, in the cylindrical coordinate system we find that

$$\mathbf{G}\Gamma = \frac{1}{4\pi}\iint_S \Gamma(\rho)\frac{\rho d\theta d\rho}{\left(\sqrt{a-b\cos(\theta-\theta_0)}\right)^3}, \quad a = \rho^2 + \rho_0^2 + (z-z_0)^2, \quad b = 2\rho\rho_0. \tag{28}$$

Rewrite the integral in eqn (28) as repeated one and introduce the inner integral as follows

$$I_1(\rho,\rho_0) = \int_{-\pi}^{\pi}\frac{d\psi}{\left(\sqrt{a-b\cos\psi}\right)^3}. \tag{29}$$

After transformations, we obtain

$$I_1(\rho,\rho_0) = \frac{4}{\sqrt{a+b}(a-b)}\int_0^{\pi/2}\sqrt{1-k_2\sin_2\psi}\,d\psi = \frac{4}{(\rho+\rho_0)(\rho-\rho_0)^2}\mathsf{E}(k), \tag{30}$$

where $\mathsf{E}(k)$ is the second kind complete elliptic integral.

Thus, we obtain one-dimensional hypersingular integral equations for determining functions $\Gamma_k(\rho)$ in the next form

$$\frac{1}{\pi}\int_0^R \Gamma_k(\rho)\frac{\rho E(k)d\rho}{(\rho+\rho_0)(\rho-\rho_0)^2} = w_k(\rho) = -\rho_l(\boldsymbol{u}_k, \mathbf{n_0}). \tag{31}$$

Note that the kernel of the integral operator in eqn (31) has Hadamard's singularity $(\rho-\rho_0)^{-2}$.

4.2 Singular integral equations

Let consider a rigid shell of revolution. Suppose that problem (26) is solved in axially symmetric formulation. Then eqn (26) can be written in the following form

$$2\pi p(\mathbf{P}_0^k) + \iint_{\Gamma_f} p\frac{\partial}{\partial\mathbf{n}}\frac{1}{|\mathbf{P}-\mathbf{P}_0^k|}d\Gamma_f = -\frac{1}{g}\iint_{\Gamma_0}\frac{\partial^2 p}{\partial t^2}\frac{1}{|\mathbf{P}-\mathbf{P}_0^k|}d\Gamma_0. \tag{32}$$

Here Γ_S is the shell wetted surface, Γ_0 is a circle. For harmonic vibrations we assume that $p(t,\mathbf{P}) = \exp(i\omega t)p(\rho,z)$. The following integral operators on a surface S with a generatrix γ are introduced [12]

$$\mathbf{A}(\sigma,S)p(\mathbf{P}) = \iint_S p(\mathbf{P})\frac{1}{|\mathbf{P}-\mathbf{P}_0|}dS = \int_\gamma p(r,z)\,\Psi(\mathbf{P},\mathbf{P}_0)d\Gamma, \quad \mathbf{P}_0 \in \sigma, \tag{33}$$

$$\mathbf{B}(\sigma,S)p(\mathbf{P}) = \iint_S p(\mathbf{P})\frac{\partial}{\partial\mathbf{n}}\frac{1}{|\mathbf{P}-\mathbf{P}_0|}dS = \int_\gamma p(r,z)\,\Theta(\mathbf{P},\mathbf{P}_0)d\Gamma, \quad \mathbf{P}\in S, \tag{34}$$

where

$$\Theta(\mathbf{P},\mathbf{P}_0) = \frac{4}{\sqrt{a+b}}\left\{\frac{1}{2r}\left[\frac{r^2-r_0^2+(z_0-z)^2}{a-b}E(k) - F(k)\right]n_r + \frac{z_0-z}{a-b}E(k)n_z\right\},$$

$$\Psi(\mathbf{P},\mathbf{P}_0) = \frac{4}{\sqrt{a+b}}F(k), \quad a = r^2 + r_0^2 + (z-z_0)^2, \quad b = 2rr_0,$$

$$F(k) = \int_0^{\pi/2}\frac{d\psi}{\sqrt{1-k^2\sin^2\psi}}, \quad E(k) = \int_0^{\pi/2}\sqrt{1-k^2\sin^2\psi}\,d\psi.$$

Let p_1 be the unknown pressure values of on the surface Γ_S, and p_0 are the pressure values on the surface Γ_0. Using eqns (33), (34) and (32), one can receive the eigenvalue problem for evaluation own modes and frequencies of the liquid in the rigid shell as follows

$$\mathbf{A}_0 p_0 = \frac{\omega^2}{g}\mathbf{B}_0 p_0. \tag{35}$$

Here $\mathbf{A}_0 = 2\pi\mathbf{I} + \mathbf{B}(\Gamma_0, \Gamma_S)\mathbf{C}^{-1}\mathbf{B}(\Gamma_S, \Gamma_0)$, $\mathbf{B}_0 = \mathbf{A}(\Gamma_0, \Gamma_0) + \mathbf{B}(\Gamma_0, \Gamma_S)\mathbf{C}^{-1}\mathbf{A}(\Gamma_S, \Gamma_0)$, $\mathbf{C} = 2\pi\mathbf{I} + \mathbf{B}(\Gamma_S, \Gamma_S)$.

Note that there are singular terms in A_0, B_0. The inner integrals in $\mathbf{A}(S,S), \mathbf{B}(S,S)$ are calculated according to the algorithm elaborated in Strelnikova et al. [12]. The external integrals in $\mathbf{A}(S,S), \mathbf{B}(S,S)$ contain logarithmical singularities.

4.3 Numerical implementation

Consider eqn (32). This is the hypersingular integral equation with the following kernel

$$K(\rho, \rho_0) = \frac{\rho \mathrm{E}(k)}{(\rho+\rho_0)(\rho-\rho_0)^2}.$$

As in Karaiev and Strelnikova [17], for more detailed elucidation of the function $K(\rho, \rho_0)$ near the singularity $(\rho - \rho_0 = 0)$, the asymptotic formula is in use for the function E(k) at k, close to 1

$$\mathrm{E}(k) = 1 + \frac{1}{2}k'^2\left(\ln\frac{4}{k'} - \frac{1}{2}\right) + \left(\frac{1}{2}\right)^2\frac{3}{4}k'^4\left(\ln\frac{4}{k'} - 1 - \frac{1}{3}\frac{1}{4}\right) + \ldots,\ k'^2 = 1 - k^2.$$

Introducing the function $K_0(\rho, \rho_0) = \frac{\rho}{(\rho+\rho_0)(\rho-\rho_0)^2}\left[1 + \frac{1}{2}k'^2\left(\ln\frac{4}{k'} - \frac{1}{2}\right)\right]$ for calculating integral (32) over the singular element l_0 we use the formula

$$\int_{l_0}\Gamma_m(\rho)K(\rho,\rho_0)d\rho = \int_{l_0}\Gamma_m(\rho)K_0(\rho,\rho_0)d\rho + \int_{l_0}\Gamma_m(\rho)\left[K(\rho,\rho_0) - K_0(\rho,\rho_0)\right]d\rho. \tag{36}$$

The first term here contains hypersingular and logarithmic components, and the second integral is non-singular. Hypersingular integrals are evaluated using their definition [16].

So then the high-precision formulas for calculating integrals with logarithmic singularities are constructed. Using the following analytical formula

$$\int_0^1 x^n \ln\frac{1}{x}dx = \frac{1}{(n+1)^2}, \tag{37}$$

we obtain quadratic formulas that exactly calculate such integrals with nodes in the roots of orthogonal polynomials with the logarithmic weight

$$\int_0^1 f(x)\ln\frac{1}{x}dx = \sum_{n=1}^{N^*} w_n f(x_n), \tag{38}$$

where w_n, x_n, and N^* are the weights, nodes, and the order of the quadrature formula.

Orthogonal polynomials with the logarithmic weight are determined by the formula

$$P_n(x) = \begin{vmatrix} 1 & \left(\frac{1}{2}\right)^2 & \left(\frac{1}{3}\right)^2 \ldots & \left(\frac{1}{n+1}\right)^2 \\ \left(\frac{1}{2}\right)^2 & \left(\frac{1}{3}\right)^2 & \left(\frac{1}{4}\right)^2 \ldots & \left(\frac{1}{n+2}\right)^2 \\ & & \ldots\ldots\ldots & \\ \left(\frac{1}{n}\right)^2 & \left(\frac{1}{n+1}\right)^2 & \left(\frac{1}{n+2}\right)^2 \ldots & \left(\frac{1}{2n}\right)^2 \\ 1 & x & x^2 \ldots\ldots & x^n \end{vmatrix}. \tag{39}$$

From eqn (39) we receive $P_0(x) = 1, P_1(x) = 4x - 1, P_2(x) = 252x^2 - 180x + 17, \ldots$ The roots of the polynomials eqn (39) are the nodes of the quadrature eqn (38). Nodal

coefficients were calculated according to Brebbia et al. [16]. Table 1 shows the values of nodes and weights for $N^* = 6$.

Table 1: Nodes and weights of quadrature formula.

n	w_n	x_n
1	0,23876366	0,021634001
2	0,30828675	0,12958339
3	0,24531742	0,31402045
4	0,14200875	0,53865721
5	0,005554622	0,75691433
6	0,010168958	0,92266884

To test the obtained quadrature, the calculation of Catalan's constant G is chosen,

$$G = \sum_{n=0}^{\infty} \frac{(-1)^n}{(2n+1)^2} = \frac{1}{1^2} - \frac{1}{3^2} + \frac{1}{5^2} - \frac{1}{7^2} + \ldots = \int_0^1 \frac{1}{1+x^2} \ln \frac{1}{x} dx. \tag{40}$$

The six-point quadrature formula gives good agreement with the analytical value G = 0.9159655941…, namely, the approximate value is $\tilde{G} = 0.9159655749$, i.e. the relative error is less than $\varepsilon = 10^{-7}$. Thus, the BEM based numerical method is elaborated for axially-symmetrical FSI problems. Singular and hypersingular integrals are reduced to one-dimensional ones, and for their evaluation the methods of treating inner integrals [17] is used, and quadrature eqn (38) for outer integrals is validated.

5 SINGULAR AND HYPERSINGULAR INTEGRAL EQUATIONS IN AXISYMMETRIC PROBLEMS

5.1 Hypersingular integral equations in evaluating pressure drop at round elastic plate immersed in water

To test the proposed method, we use the analytical solution $\Gamma(x, y) = \sqrt{R^2 - x^2 - y^2}$ of the 3D hypersingular integral equation

$$\frac{1}{\pi} \iint_S \frac{\Gamma(x,y)dxdy}{\sqrt{(x-x_0)^2+(y-y_0)^2}^3} = -\pi, \quad S = \{(x, y): x^2 + y^2 \le R^2\}. \tag{41}$$

Using (41), for the one-dimensional equation in the form

$$\frac{1}{\pi} \int_0^R \Gamma(\rho) \frac{\rho \mathsf{E}(k) d\rho}{(\rho + \rho_0)(\rho - \rho_0)^2} = -1, \tag{42}$$

we obtain the next analytical solution

$$\Gamma(\rho) = \frac{4}{\pi} \sqrt{R^2 - \rho^2}. \tag{43}$$

Numerical solution of eqn (42) is obtained using the method described above. It is supposed that $R = 1$ m. The comparison of numerical and analytical results is given in Fig. 2(a).

Here, the solid line corresponds to the analytical solution, the points indicate the numerical data. The number of boundary elements with constant approximation of the density is equal to 100. Note that accuracy $\varepsilon = 10^{-4}$ is obtained at almost all points of the segment $[0, R]$ except

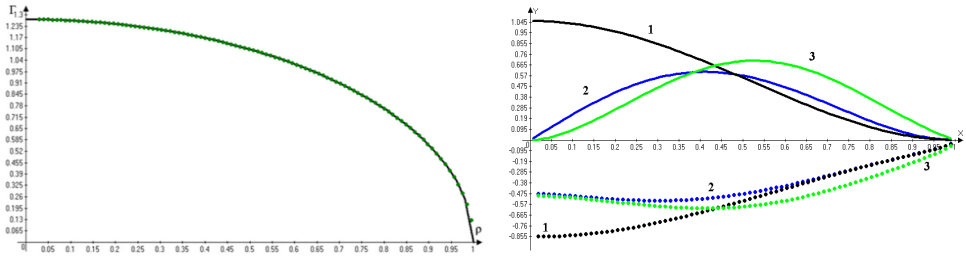

(a) (b)

Figure 2: Solutions of hypersingular integral equations.

for points near the ends of the interval. As far as ρ, ρ_0 are close to zero, an additional singularity arises in eqn (42), and it is proposed in Brebbia et al. [16] to replace the integration segment by $[\delta, R]$. Here $\delta = 0.025/R$ is chosen. If ρ is close to 1, the accuracy can be increased by taking into account the solution behavior at the ends of the integration interval. Note that BEM for the two-dimensional region in Chantarawichit and Sompornjaroensuk [18] used 1200 boundary elements, and the obtained accuracy is $\varepsilon=10^{-4}$. These data indicate the effectiveness of the proposed method.

Next, numerical solutions of eqn (31) with following right-hand parts

$$w_k(\rho) = \mathrm{J}_0(\alpha_k\rho) - \frac{\mathrm{J}_0(\alpha_k R)}{\mathrm{I}_0(\alpha_k R)}\mathrm{I}_0(\alpha_k\rho), \tag{44}$$

are obtained. Eqn (44) are own modes of vibrations of dry circle elastic plate with radius R. Fig. 2(b) shows the functions $w_k(\rho)$ and corresponding to them solutions $\Gamma_k(\rho), k = 0,1,2$ of hypersingular integral eqn (31). Here, numbers 1–3 correspond to $k = 0,1,2$, the dashed lines represent the right parts $w_k(\rho)$, and the solid lines correspond to the functions $\Gamma_k(\rho)$.

5.2 Singular integral equations in evaluating frequencies and modes of shells of revolution

Modes and frequencies of free liquid vibrations for conical, spherical and cylindrical rigid shells (Fig. 3) are evaluated by solving eigenvalue problem eqn (35) using proposed BEM for numerical implementation of singular integral eqn (32). It is supposed that R=1m, H=1m, for all shells under consideration, and R_1=0.5m for truncated conical shell.

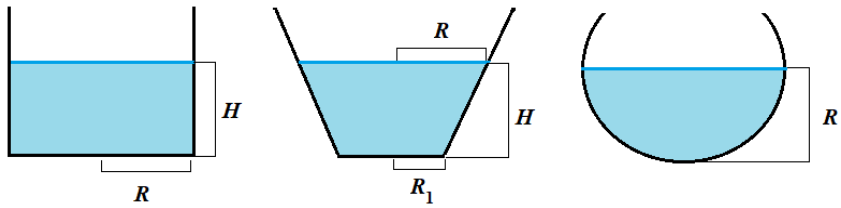

Figure 3: Drafts of cylindrical, conical, and spherical fluid-filled shell.

The axisymmetric linear sloshing is considered. The total number of boundary elements along shell meridians and radii of free surfaces is 240 for all shells in BEM implementation.

A comparison of results for axisymmetric modes is shown in Table 2.

Table 2: Frequency parameter ω^2/g for different shells.

k	Conical shell	Spherical shell	Cylindrical shell	
	Numerical solution	Numerical solution	Numerical solution	Analytical solution
1	3.4665	3.7456	3.8281	3.8281
2	6.6810	6.9763	7.0160	7.0159
3	9.8453	10.1474	10.1732	10.1734
4	12.9911	13.3041	13.3334	13.3236

The analytical solution is expressed in the next form [19]:

$$\frac{\omega_k^2}{g} = \frac{\mu_k}{R}\tanh\left(\mu_k \frac{H}{R}\right),\ k = 1,2,..;\varphi_k = \mathrm{J}_0\left(\frac{\mu_k}{R}r\right)\cosh\left(\frac{\mu_k}{R}z\right)\cosh^{-1}\left(\frac{\mu_k}{R}H\right), \qquad (46)$$

where μ_k are roots of the equation $\mathrm{J}_0'(x) = 0$, $\mathrm{J}_0(x)$ is the first kind Bessel function, ω_k, φ_k are frequencies and modes of liquid sloshing in the rigid cylindrical shell.

The results of Table 2 testify convergence of proposed BEM. The accuracy $\varepsilon = 10^{-4}$ has been achieved. The lowest frequencies correspond to truncated conical shell.

Fig. 4 demonstrates distributions of first three sloshing modes on the free surface. The solid lines denote modes obtained by analytical expression (46) at $z = H$. The lines pointed with circles and squares denote numerical solutions.

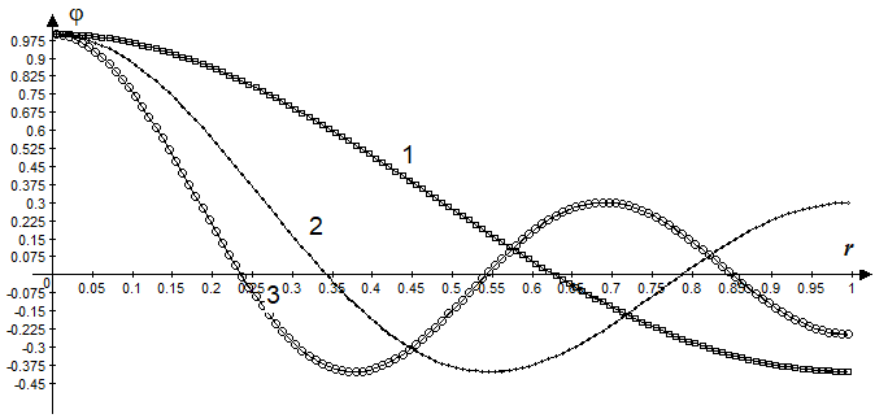

Figure 4: Numerically and analytically obtained modes.

Sloshing modes are the same for conical, spherical and cylindrical shells and have the Bessel-like behaviour. Generalization of the developed method for non-axisymmetric vibrations can be carried out using the approach from Gnitko et al. [20].

6 CONCLUSION

The boundary element method is used to solve singular and hypersingular integral equations arising in FSI problems. The hypersingular equations appear in FSI problems considering thin structural elements completely immersed in liquid. Singular integral equations are

specific to FSI analysis of shell structures partially filled with fluids. The common feature of all these problems is the possibility of reducing them to one-dimensional equations in axisymmetric formulation. This was done by integrating over the circumferential coordinate. It was proved that the inner integrals are elliptic integrals and their combinations, while the outer ones have hypersingular and logarithmic singularities. The effective numerical procedures are developed for calculating both inner and outer integrals with high accuracy. Numerical simulation was carried out. The proposed method significantly reduces the computer time for vibration analysis and reveals new qualitative possibilities in modeling the dynamic behavior of shells and plates interacting with liquids.

ACKNOWLEDGEMENT

The authors gratefully acknowledge Professor Alexander Cheng for his constant support and interest to our research.

REFERENCES

[1] Trivedi, C. & Cervantes, M.J., Fluid-structure interactions in Francis turbines: A perspective review. *Renewable and Sustainable Energy Reviews*, **68**, pp. 87–101, 2017.

[2] Iovănel, R.G., Dunca, G., Bucur D.M. & Cervantes M.J., Numerical simulation of the flow in a Kaplan turbine model during transient operation from the best efficiency point to part load. *Energies*, **13**(12), p. 3129, 2020. DOI: 10.3390/en13123129.

[3] Rusanov, A., Shubenko, A., Senetskyi, O., Babenko, O. & Rusanov, R., Heating modes and design optimization of cogeneration steam turbines of powerful units of combined heat and power plant. *Energetika*, **65**(1), pp. 39–50, 2019.

[4] Grinderslev, C., Sørensen, N.N., Horcas, S.G., Troldborg N. & Zahle, F., Wind turbines in atmospheric flow: Fluid–structure interaction simulations with hybrid turbulence modelling. *Wind Energy Science*, **6**, pp. 627–643, 2021.

[5] Avramov, K.V., Nonlinear vibrations characteristics of single-walled carbon nanotubes via nonlocal elasticity. *International Journal of Nonlinear Mechanics*, **107**, pp. 149–160, 2018. DOI: 10.1016/j.ijnonlinmec.2018.08.017.

[6] Gnitko, V., Marchenko, U., Naumenko, V. & Strelnikova, E., Forced vibrations of tanks partially filled with the liquid under seismic load. *Proceedings of the XXXIII Conference on Boundary Elements and Other Mesh Reduction Methods, Transactions on Modelling and Simulation,* WIT Press: Southampton and Boston, vol. 52, pp. 285–296, 2011. DOI: 10.2495/BE110251.

[7] Mansouri, A. & Aminnejad, B., Investigation of oil reservoir vibration under the impact of earthquake in proper and corrosion-occurred tanks. *American Journal of Civil Engineering and Architecture*, **1**, pp. 181–199, 2013.

[8] Faltinsen, O.M., Lagodzinskyi, O.E. & Timokha, A.N., Resonant three-dimensional nonlinear sloshing in a square base basin. Part 5. Three-dimensional non-parametric tank forcing. *Journal of Fluid Mechanics*, **894**, A10, pp. 1–42, 2020. DOI: 10.1017/jfm.2020.253.

[9] Strelnikova, E., Kriutchenko, D., Gnitko, V. & Degtyarev, K., Boundary element method in nonlinear sloshing analysis for shells of revolution under longitudinal excitations. *Engineering Analysis with Boundary Elements*, **111**, pp. 78–87, 2020. DOI: 10.1016/j.enganabound.2019.10.008.

[10] Zhou-Bowers, S. & Rizos, D.C., B-spline impulse response functions of rigid bodies for fluid-structure interaction analysis. *Advances in Civil Engineering*, Corpus ID: 56357618, 2018. DOI: 10.1155/2018/9760361.

[11] Boyko, E., Bercovici, M. & Gat, A.D., Viscous-elastic dynamics of power-law fluids within an elastic cylinder. *Physical Review Fluids*, **2**, 073301, 2017.
[12] Strelnikova, E., Choudhary, N., Kriutchenko, D., Gnitko, V. & Tonkonozhenko, A., Liquid vibrations in circular cylindrical tanks with and without baffles under horizontal and vertical excitations. *Engineering Analysis with Boundary Elements*, **120**, pp. 13–27, 2020. DOI: 10.1016/j.enganabound.2020.07.024.
[13] Saghi, R., Hirdaris, S. & Saghi, H., The influence of flexible fluid structure interactions on sway induced tank sloshing dynamics. *Engineering Analysis with Boundary Elements*, **131**, pp. 206–217, 2021. DOI: 10.1016/j.enganabound.2021.06.023.
[14] Smetankina, N., Kravchenko, I., Merculov, V., Ivchenko, D. & Malykhina, A., Modelling of bird strike on an aircraft glazing. *Integrated Computer Technologies in Mechanical Engineering*, eds M. Nechyporuk, V. Pavlikov & D. Kritskiy, Springer: Cham, pp. 289–297, 2020. DOI: 10.1007/978-3-030-37618-5_25.
[15] Huang, W.-X. & Tian, F.-B., Recent trends and progress in the immersed boundary method. *Proceedings of the Institution of Mechanical Engineers, Part C: Journal of Mechanical Engineering Science*, **233**(23–24), pp. 7617–7636, 2019.
[16] Brebbia, C.A., Telles, J.C.F. & Wrobel, L.C. (eds), *Boundary Element Techniques*, Springer-Verlag: Berlin and New York, 1984.
[17] Karaiev, A. & Strelnikova, E., Axisymmetric polyharmonic spline approximation in the dual reciprocity method. *Zeitschrift für Angewandte Mathematik und Mechanik*, **101,** e201800339. 2021. DOI: 10.1002/zamm.201800339.
[18] Chantarawichit, P. & Sompornjaroensuk, Y., Vibration of circular plates with mixed edge conditions. *ITK Research Journal*, **14**(2), pp. 136–156, 2020.
[19] Ibrahim, R.A., *Liquid Sloshing Dynamics. Theory and Applications*, Cambridge University Press, 2005.
[20] Gnitko, V., Karaiev, A., Choudhary, N. & Strelnikova, E., Boundary element method analysis of boundary value problems with periodic boundary conditions. *WIT Transactions on Engineering Sciences*, vol. 131, pp. 31–44, 2021. DOI: 10.2495/BE440031.